

Thermal Performance Investigation on Corrugated Plate Heat Exchangers

Benny. T. K¹, Akhil. A², Devakrishna³, Ramzy. R⁴, Sinan. T⁵

¹Asst. Professor, Department of Mechanical Engineering, RIET, Thiruvananthapuram, Kerala, India

²⁻⁵UG Student, Department of Mechanical Engineering, RIET, Thiruvananthapuram, Kerala, India

Abstract - Compact heat exchangers have become an essential necessity for power production and other purposes on a daily basis. The corrugated plate exchangers (CPHE) are well known for their high thermal performance. The overall tests have been conducted on CPHEs for two symmetric chevron angles (β) of $50^\circ/50^\circ$, $60^\circ/60^\circ$ and $70^\circ/70^\circ$. Data are obtained for steady state, single phase (water-water), counter arrangements, and for Reynolds number (Re) ranges from 500 to 2500, sophisticated mesh technique have been adopted to develop the mesh for the plates and the fluid between the plates. An appropriate grid refinement test has been carried out for the accuracy of the numerical results. The result has been validated through numerical data. A realizable $k - \epsilon$ turbulence model with scalable wall treatment found to provide the most consistent and accurate prediction of the thermal performance of CPHE. The numerical result showed that the effectiveness of the CPHE $50^\circ/50^\circ$ is higher than both $60^\circ/60^\circ$ and $70^\circ/70^\circ$ but the CPHE $70^\circ/70^\circ$ shows higher Nusselt value than other two.

Okada et al. [8], investigated the impact of different β on CPHE's thermal performance, where β was considered with horizontal line, but it was common β to be considered with respect to vertical line as shown in Fig -1. Later Muley and Manglik [9] studied heat transfer characteristics (HTC) in CPHE for $\beta = 30^\circ/30^\circ$, $60^\circ/60^\circ$ and $30^\circ/60^\circ$. Never the less each correlation to be separated, for the whole study were incorporated in one formula. Khan et. Al. [10] carried out a one-one pass, water-water fluids for the same β 's, and found out that, the same Re on the both sides of the CPHE does not imply heat transfer co-efficient (h) will be the same, as h depends on many other factors such as fluid viscosity, fluid density, fluid velocity and many other parameters.

Key Words: Corrugated plate heat exchanger, Thermal performance, Nusselt number, Chevron, Computational fluid dynamics.

1.INTRODUCTION

A heat exchanger is a device that is used to transfer thermal energy (enthalpy) between two or more fluids, between a solid surface and a fluid, or between solid particulates and a fluid, at different temperatures and in thermal contact. In heat exchangers, there are usually no external heat and work interaction. The CPHE is the most efficient comparing to other conventional type heat exchangers. The efficiency of the heat exchanger increases in fluid contact surfaces, pressure drop and mass flow rates due to enhanced heat transfer to the fluid [1]. Many researches have studied different approaches to enhance flow mixing and heat transfer by introducing passive techniques to control the energy dissipation rate and enhance turbulence intensity [2-4]. Corrugated Plate Heat Exchanger (CPHE) are compact, provides high thermal effectiveness and close approach temperatures (up to 2°C difference) can be obtained [5].

CPHEs are lighter and require less space. So, they have been employed in food, power, HVAC and many other applications [6]. In CPHEs, the turbulent flow can be achieved at low Reynolds Number (Re), $Re > 400$ [7].

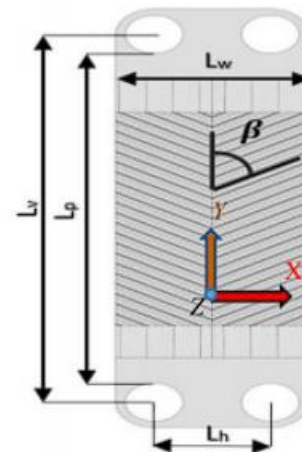


Fig -1: Geometrical Parameters illustration for chevron type plates.

The experimental and numerical studies have concluded that the flow inside the CPHE is non-uniform and tends to flow towards the lateral edges of the plate but does not consider the thermal performance [11]. A two symmetric $\beta = 30^\circ/30^\circ$ and $60^\circ/60^\circ$ CPHEs were numerically studied using CFD by Asif et al. [12]. The thermo-hydraulic characteristics was investigated in the form of Nusselt number. The essential details were not provided for supporting the type of adopting turbulence model, and no information of the number of channels or plates.

Saha S.K et al [13], investigated thermal performance on cross corrugated plate heat exchanger and found that corrugations improve both flow distribution and heat transfer in the PHE. The friction factor decreases with the increase in Reynolds number at a fixed corrugation angle, whereas the friction factor increases with increasing corrugation angle at a given Re . Ming Chen et al [14],

investigated pressure and flow distribution on chevron corrugated plate heat exchanger and found that, as the fluid enters the degree of fluid turbulence is increased and the temperature gradient as well as the pressure gradient increases towards the outlet. Since there exist a large number of contact point result in even fluid distribution. Sanjeev Jain et al [15], performed a numerical simulation of small sized chevron plate heat exchanger and found out that the numerical friction factor values (8%-33%) and Nusselt number (3% - 18%) underpredicted due to the exclusion of ports and its flow distribution area.

One good aspect of considering CFD study comparing to experimental model is that, it enables to find the temperature at any spot on the model, and the average temperature for any side of the plate. Consequently, h can directly be calculated from numerical data. An essential objective of the present study is to introduce the optimum design turbulent angle in a chevron plate for the enhance thermal performance for the current CPHE. Jonghyeok Lee et al [16], investigated the flow characteristics and thermal performance in chevron type plate heat exchanger and found that, both friction factor (f) and Colburn factor (j) increased as β increased and as Chevron pitch to Chevron height ratio (p/h) decreased. We found that JF was the largest with β 30° for laminar flow, and with β 60° for turbulent flow and for a fixed p/h , JF was almost constant with Reynolds number (Re). S. Islam et al [17], investigated the thermal performance between the newly designed flow arrangements to that of a conventional corrugated plate heat exchanger and found out that the Calculated Nu for newly designed β $60^\circ/60^\circ$ CPHE is up to 75% higher than that of the existing β $60^\circ/60^\circ$ CPHE. G. Kanaris et al [18], investigated the flow and heat transfer in a narrow-corrugated channel and explains the ability of CFD code to predict the flow and heat transfer in small 5 channels. The simulation results reveal that, compared to a smooth-wall plate heat exchanger, corrugations improve both flow distribution and heat transfer.

The present study introduces a new modification in CPHE flow mechanism as described in the following section, which could enhance convective heat transfer significantly between the cold and the hot fluids, and consequently the fuel consumption can be reduced [19]. The numerical thermo-hydraulic performance tests carried out on counter-current flow arrangement, for two symmetric $\beta = 30^\circ/30^\circ$, and $60^\circ/60^\circ$. Nu is employed as an indicator for heat transfer improvement, and CPHE effectiveness (\mathcal{E}) is employed to compare the thermal performance between the basic and the new CPHE design. The CPHE comprised of four channels (five plates), two of them are pertaining to the cold side, which represent the utility fluid, and the other two pertaining to the hot side, which represent the product fluid. Therefore, the present study is performed on the hot side of CPHE. The corrugations shape have been considered for all cases in order to get as closer as possible to simulate thermal-hydraulic performance in real CPHE.

2. NUMERICAL METHOD

2.1 Turbulence Model

ANSYS FLUENT provides a large selection of turbulence models, however, care must be taken during choosing an appropriate model. The most common turbulence model that is considered as an industry standard model is $k - \epsilon$ model. On the other hand, the shear stress transport (SST) $k - \omega$ turbulence model is also used to simulate some heat transfer processes. The SST $k - \omega$ model is the combination of $k - \omega$ and standard $k - \epsilon$ and can resolve the boundary layers near the wall, whereas, the standard $k - \epsilon$ model can resolve the boundary layer away from the wall.

The realizable $k - \epsilon$ model [20] is relatively new approach that differs from standard one. It shows an outstanding accuracy to capture the mean flow for a very complicated structure. A realizable $k - \epsilon$ model satisfies a specific mathematical constraint as well as complied with turbulent flow physics. In addition, a realizable $k - \epsilon$ model can provide a superior performance for simulating complex flows, that includes boundary layer reattachment, circulation, rotation, and strong adverse pressure gradient.

Generally, all turbulence models have been tested for this problem. The realizable $k - \epsilon$ model has been adopted. Because it showed the most accurate result that is close to the experimental one as well as its consistency with different Re .

2.2 Governing Equations

For the Reynolds number considered here, fluid inside CPHEs are subjected to turbulent flow due to the change in velocity in the corrugations of chevron plates. The heat transfer takes place between the cold and hot side and consequently a transition of physical properties such as temperature, pressure, viscosity, density and velocity. Therefore Navier-Stokes Eq. (NS) (1) is used to estimate changes on these properties during the thermal and dynamic interaction as shown below:

$$\frac{\partial}{\partial x_j} (\rho u_i u_j) = -\frac{\partial p}{\partial x_j} + \frac{\partial}{\partial x_j} \left[(\mu + \mu_t) \frac{\partial u_i}{\partial x_j} \right] \quad (1)$$

Here, NS can be considered as Newton's second law applied to estimate pressure, inertia and viscous force along the fluid motion. ANSYS FLUENT solves these equations along with continuity Eq. (2) and refers to conservation of mass whereas NS refers to momentum conservation.

$$\frac{\partial}{\partial x_i} (\rho u_i) = 0 \quad (2)$$

The energy equation is included to resolve the heat transfer among the cold fluid, the hot fluid and the plate as shown in Eq. (3):

$$\rho C_p \frac{\partial y}{\partial x} (u_j T) = k_{eff} \frac{\partial^2 T}{\partial x_j^2} + (T_{if})_{eff} \frac{\partial u_i}{\partial x_j} \quad (3)$$

The finite volume based technique is used to discretize the governing Eqs. Along with second order and first order upwind scheme to discretize the convection term, the turbulent kinetic energy and dissipation rate.

2.3 Data Formulation

In the study, *Re* set as the same for both hot and cold fluids inside the flow channels. However, *Nu* was not considered to be the same.

$$Re = \frac{m' d_e}{\mu A_e N} \quad (4)$$

m' is calculated to meet the required *Re*. Here *Re*, μ , *N*, *A_e* and *d_e* are known, whereas *d_e* is twice the plate's corrugation depth.

The fluid's inlet temperatures and mass flow rate have been set in as the initial boundary conditions. The required measurements are the outlet temperatures of cold and hot fluids as well as the hot walls temperature. The heat transfer data are been expressed using the employed two main non-dimensional parameters where *Nu* is used as a scale heat transfer improvement and ϵ is calculated to compare the thermal performance between the three symmetrical chevron β 50°/50°, β 60°/60° and β 70°/70°. The hot side of fluid is considered for *Nu* and ϵ since hot side is the product fluid and cold side is the utility side.

Nu is given by:

$$Nu = \frac{h_h d_e}{k} \quad (5)$$

Where the *k* is thermal conductivity of hot water. The heat transfer coefficient, *h_h* is calculated as follows:

The hot heat load is given by:

$$Q_h = m'_h c_{p,h} (T_{h,i} - T_{h,o}) \quad (6)$$

and cold heat load is given by:

$$Q_c = m'_c c_{p,c} (T_{c,o} - T_{c,i}) \quad (7)$$

c_{p,h} and *c_{p,c}* has been extracted from the tables of thermodynamics at hot and cold fluid bulk mean temperatures as follows:

The hot fluid bulk mean temperature is given by:

$$T_{h,b} = \frac{(T_{h,i} + T_{h,o})}{2} \quad (8)$$

And cold fluid bulk mean temperature is given by:

$$T_{c,b} = \frac{(T_{c,i} + T_{c,o})}{2} \quad (9)$$

Note; To fulfill the energy balance, the difference between *Q_h* and *Q_c* should always be zero. However, the difference of about 95% of the simulations is less than $\pm 4-5\%$, and $\pm 7-9\%$ for the rest of the simulations. Therefore, *Q_{avg}* is taken as the average value of the hot and cold heat load and considered for the current calculations.

$$Q_{avg} = \frac{Q_h + Q_c}{2} \quad (10)$$

So, *h_h* is given by:

$$h_h = \frac{Q_{avg}}{A(T_{h,b} - T_{w,h})} \quad (11)$$

Hence, *Nu* can be evaluated.

Q_{avg} is the maximum possible amount of heat that could be exchanged between hot and cold fluids and is given by:

$$Q_{avg} = C_{min} (T_{h,i} - T_{c,i}) \quad (12)$$

C_{min} is the minimum heat capacity. For all the cases in the current study *C_h* < *C_c*:

Then, ϵ is determined as:

$$\epsilon = Q_{avg} / Q_{min} \quad (13)$$

3. ANALYSIS MODEL SETUP

3.1 CAD Geometry Design

Three CPHEs model are drawn using Solidworks 2020. Three symmetric CPHEs with β 50°/50°, β 60°/60° and β 70°/70° are developed according to the basic plate design procedures.

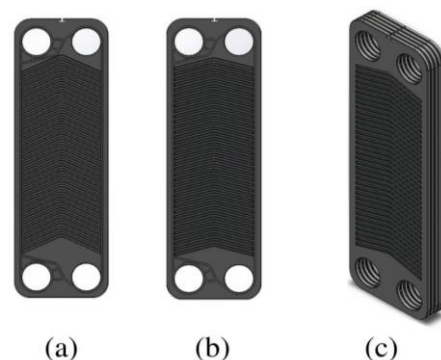


Fig -2: Front plane view of (a) β 50°/50°, (b) β 70°/70° plate and (c) trimetric view of the CPHE model having β 60°/60°.

Each CPHE consists of five plates, which generates four flow channels where alternatively two channels belong to the hot and other two for the cold side. In order avoid gasket rub off effect, small gasket hold engravement are provided in the

plate design. All geometric parameters have been developed carefully, thus the corrugations have a sinusoidal shape similar to that of the industrial applied ones.

3.2 Meshing and Optimization

The CPHE contains a large number of curves and angled narrow passages. To obtain better analysis results, adequate mesh elements in these small passages to be ensure. An unstructured tetrahedron mesh elements are adopted with an advance technique for good quality mesh. Patch conforming and patch independent algorithms are enabled for the same geometry. The patch conforming is a Delaunay mesher, where mesh refinement is carried out by using front point insertion and meshing uses the bottom up approach from edges to volume in sequence. On the other hand, patch independent is based on spatial subdivision and mesh refinement is carried out where necessary. Large mesh elements are produced where possible thus allowing for faster computation. The meshing process prefers to be top down approach; that is, volume mesh is carried first and then surface mesh is created by projecting volume mesh to faces and edges.

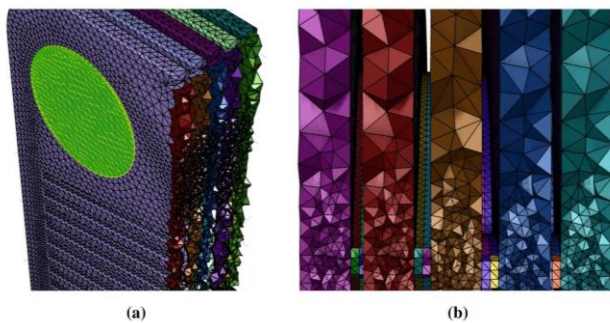


Fig -3: (a) Trimetric view of meshed model having β 60° chevron plate and (b) close right side view of β 70° meshed model.

Sample of the mesh is shown in Fig -3 (a) and (b). To ensure solution stability, the mesh dependency test have been carried out for each model as shown in Table -1. Mesh elements of 4.1 lakh for β 50°/50°, mesh elements of 4.2 lakh for β 60°/60° and mesh elements of 4.4 lakh for β 70°/70° have been adopted, respectively.

3.3 Boundary Conditions and Material Properties

The working fluid is water-water and counter flow arrangements. Both hot and cold fluids inlet boundary conditions are set as velocity inlet. The mass flow rate is calculated as per Eq. (4) to meet the required Re value. Thus, velocity-inlet can be calculated from inlet mass flow rate. The hot and the cold inlet water temperatures are set to 40 °C and 18 °C respectively. The fluids thermodynamic properties (ρ , c_p , k_f and μ) have been set for each fluid according to its temperature.

Zero-gauge pressure is set on both cold and hot outlets. The conjugate heat transfer is enabled where plate thickness

is set to 0.5 mm and the optimum value for turbulence intensity for current flow pattern is 5% as per Ansys Fluent user manual. Stationary and no slip conditions are set for all walls. Since, all studies performed on CPHE have used stainless steel, it is adopted as the plate material whereas high-grade Teflon is opted for gasket. The plate's ρ , c_p and k are 8030 kg/m³, 502.48 J/kg.K and 16.27 W/m.k, respectively as been defined.

Table -1: Mesh independent test for β 50° and β 70° CPHE

CPHE Type (β)	Mesh Elements (Lakhs)	Outlet cold average temperature (K)	Outlet hot average temperature (K)
β 50°/50° CPHE	3.6	298.44	309.13
	4.1	298.73	309.62
	4.7	298.95	309.87
β 60°/60° CPHE	3.5	297.22	310.94
	4.2	297.51	311.13
	4.8	297.86	311.37
β 70°/70° CPHE	3.8	296.17	312.22
	4.4	296.32	312.54
	4.9	296.58	312.63

4. RESULT AND DISCUSSIONS

In the present study, three symmetric CPHEs have been employed. All three are belonging to the well-known basic plate design with $\beta = 50^\circ/50^\circ$, $60^\circ/60^\circ$ and $70^\circ/70^\circ$. The numerical simulation are been carried out for the single phase water-water. Reynolds number from 500 to 2500. All three CPHEs have identical geometrical (b , d_e and A_e) dimension and physical (T_{hi} , T_{ci} and Re) conditions.

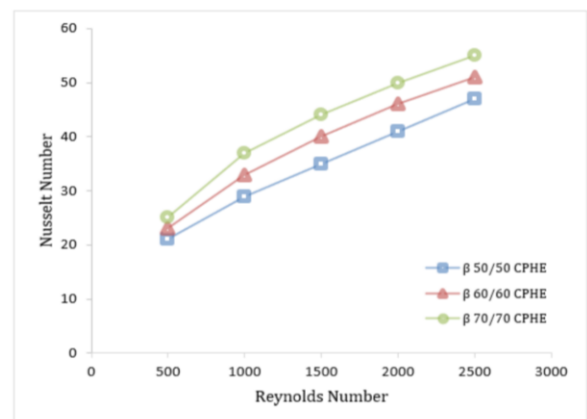


Fig -4: Nu values versus Re for all chevron CPHEs.

Table -2: Comparison between Nu of all CPHEs

Re	Nu β 50°/50° CPHE	Nu β 60°/60° CPHE	Nu β 70°/70° CPHE
500	21.7	24.3	26.4
1000	30.1	31.8	32.6
1500	38.6	38.2	40.8
2000	42.2	44.5	49.3
2500	48.9	51.7	55.8

Nusselt number has been calculated for all CPHEs as shown in Fig -4. The result shows that, Nu is directly proportional to the plate's chevron angle as well as the Re . In addition, the higher chevron angle exhibits significant heat transfer enhancement for all cases. At the same Reynolds number, Nusselt number for β 70°/70° increases up to 22% compare to the β 50°/50° as per Table -2.

The non-uniformity of the CPHEs surfaces causes velocity fluctuation. The fluid has the maximum velocity at the corrugation's ridges and the minimum velocity at the corrugation's furrows. This fluctuation of velocity causes disruption and secondary flow development. Higher the chevron angle as much higher the velocity fluctuation, consequently provide higher heat transfer enhancement.

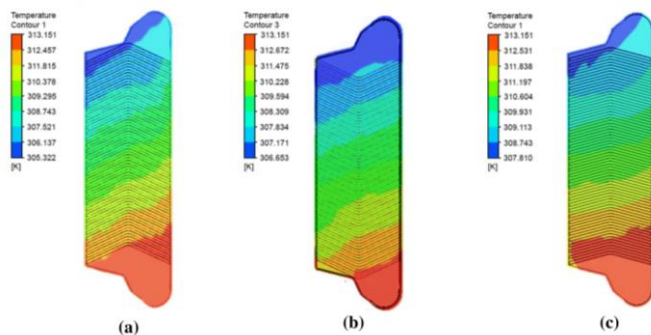


Fig -5: For Re 500, temperature contour for CPHE having (a) β 50°/50°, (b) β 60°/60° and (c) β 70°/70°.

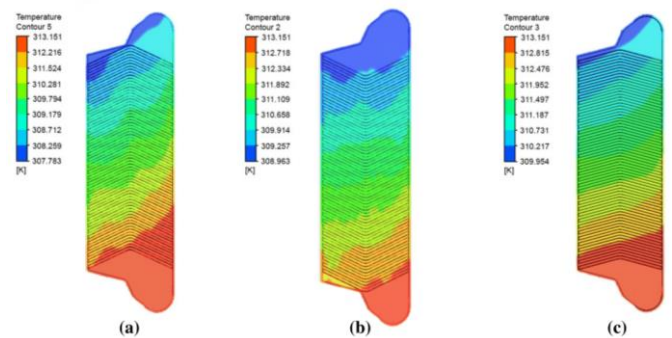


Fig -6: For Re 2500, temperature contour for CPHE having (a) β 50°/50°, (b) β 60°/60° and (c) β 70°/70°.

Fig - 5 and Fig -6 shows the temperature contour on the hot channel that locates at the middle (as shown in Fig -7) of the CPHEs. The hot water inlets in the bottom right and outlets through top right. Thus, the temperature distribution refers high temperature zones in the bottom right indicated in red color where as low temperature zones in top right, showing that the temperature gets reduced as it flows in the channel.

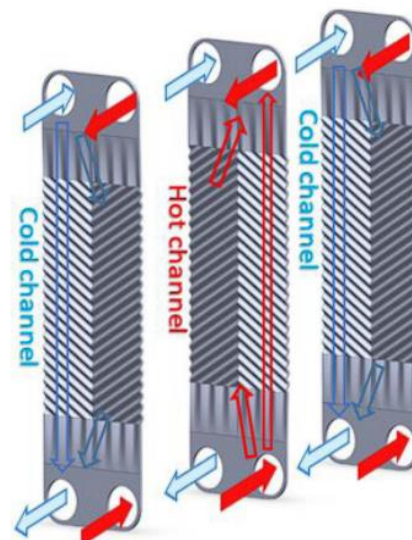


Fig -7: Schematic illustration for flow arrangement in CPHEs

For all the cases, the temperature of the last hot channel is higher than that of the first hot channel. Since, the last hot channel transfers heat with cold fluid from one side only (the side that locates just before the last channel). The first hot channel transfers heat with cold from both the front and back sides. Therefore, its temperature is always less than the last channel.

In addition, the hot fluid's temperature shows less homogeneity as the increase in chevron angle. The temperature of CPHEs hot fluid on the left side is lower than that on the right side as shown in Fig -5 and Fig -6. That is because the cold fluid is entering from the left side in the fore and the next adjacent cold channel as shown in Fig -7.

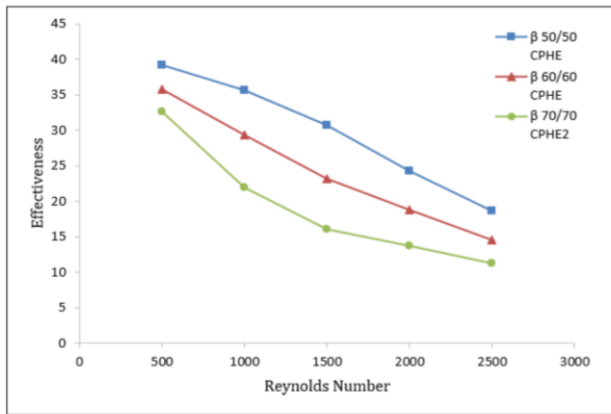


Fig -8: Comparison of ϵ values versus Re for all CPHEs.

Thermal performance of three CPHEs has been calculated in the form of CPHE's effectiveness (ϵ). Fig -8 shows the CPHE's ϵ versus Reynolds number for all the cases. In addition, quantitative data of the ϵ for all the cases of Reynolds number is given in Table -3.

Table -3: Comparison between ϵ of all CPHEs to varying Re .

Re	ϵ β 50°/50° CPHE	ϵ β 60°/60° CPHE	ϵ β 70°/70° CPHE
500	39.2	35.8	32.6
1000	35.6	29.3	21.9
1500	30.7	23.2	16.1
2000	24.3	18.8	13.8
2500	18.7	14.5	11.3

The maximum effectiveness is obtained at the lower Reynolds number for all the CPHE. CPHE having $\beta 50^\circ/50^\circ$ shows more effectiveness compared to CPHE $\beta 60^\circ/60^\circ$ and that of CPHE $\beta 70^\circ/70^\circ$. From the result the effectiveness reduces with increase in Re this relates to effectiveness reduces with increase in mass flow rate because mass flow rate is proportional to Re also mass flow rate is proportional to velocity of flow this concludes the effectiveness reduces with increase in velocity.

5. CONCLUSIONS

Thermal performance of CPHE for symmetric $\beta = 50^\circ/50^\circ, 60^\circ/60^\circ$ and $70^\circ/70^\circ$ has been carried out. A realizable $k - \epsilon$ turbulence model with scalable wall treatment found to provide the consistent and accurate results of the thermal performance. The numerical

simulations have been conducted for steady state single phase (water- water) and counter flow arrangement.

The CFD results showed that, the thermal performance of the CPHE $\beta 50^\circ/50^\circ$ is significantly higher than that of CPHE $\beta 60^\circ/60^\circ$ and $\beta 70^\circ/70^\circ$. For the CPHE $\beta 70^\circ/70^\circ$, the calculated Nu is 22% higher where as CPHE $\beta 60^\circ/60^\circ$ is 10% higher than that of CPHE $\beta 50^\circ/50^\circ$. The effectiveness for the CPHE $\beta 50^\circ/50^\circ$ is 4% and 9% higher than that of CPHE $\beta 60^\circ/60^\circ$ and $\beta 70^\circ/70^\circ$ respectively.

This study would increase the understanding of the thermal behavior of the CPHE at higher turbulency conditions. The finding of the present study suggests that the use of CPHE $\beta 50^\circ/50^\circ$ is more applicable and efficient in industries especially in industries where a high heat recovery is needed. Further studies can be done on the present study by either changing the geometrical dimensions of the CPHE or changing other factors in order to get maximum efficiency for heat exchangers.

ACKNOWLEDGEMENT

The authors would like to thank the high-performance computing system in Sinxign, Thiruvananthapuram, Kerala.

REFERENCES

- [1] G. Biswas and K. Torii, "Numerical and experimental determination of flow structure and heat transfer effects of longitudinal vortices in a channel flow", Int. J. Heat Mass Transf. 39 (16) (1996) 3441-3451.
- [2] A. Sinha and K.A. Raman, "Effects of different orientations of winglet arrays on the performance of plate-fin heat exchangers", Int. J. Heat Mass Transf. 57 (1) (2013) 202-214.
- [3] P. Saha and S. Sarkar, "Comparison of winglet-type vortex generators periodically deployed in a plate-fin heat exchanger - a synergy based analysis", Int. J. Heat Mass Transf. 74 (2014) 292-305.
- [4] T. Rush and T. Newell, "An experimental study of flow and heat transfer in sinusoidal wavy passages", Int. J. Heat Mass Transf. 42 (9) (1999) 1541-1553.
- [5] Z.H. Ayub, "Plate heat exchanger literature survey and new heat transfer and pressure drop correlations for refrigerant evaporators", Heat Transf. Eng. 24 (5) (2003) 3-16.
- [6] M. Young, "Plate heat exchangers as liquid cooling evaporators in ammonia refrigeration system", Proceeding of the IIAR Sixteenth Annual Meeting, 1994.
- [7] R.K. Shah and D.P. Sekulic, "Fundamentals of Heat Exchanger Design", John Wiley & Sons, 2003.
- [8] K. Okada and M. Ono, "Design and heat transfer characteristics of new plate heat exchanger", Heat Transf. Jpn. Res. 1 (1) (1972) 90-95.
- [9] A. Muley and R. Manglik, "Experimental study of turbulent flow heat transfer and pressure drop in a plate heat exchanger with chevron plates", J. Heat Transf. 121 (1) (1999) 110-117.

- [10] T. Khan and M. Khan, "Experimental investigation of single-phase convective heat transfer coefficient in a corrugated plate heat exchanger for multiple plate configurations", *Appl. Therm. Eng.* 30 (8-9) (2010) 1058–1065.
- [11] A. Lozano and F. Barreras, "The flow in an oil/water plate heat exchanger for the automotive industry", *Appl. Therm. Eng.* 28 (10) (2008) 1109–1117.
- [12] M. Asif and P. Muizz, "Simulation of corrugated plate heat exchanger for heat and flow analysis", *Int. J. Heat Technol.* 35 (1) (2017) 205–210.
- [13] Sandip K. Saha and Abdul Harris Khan., "Numerical study on the effects of corrugation angle on thermal performance of cross corrugated plate heat exchangers", Department of Mechanical Engineering, IIT Bombay, *Thermal science and engineering progress* 20 (2020) 19071.2020.
- [14] Shao-jie chen and Qin wang, "A numerical and experimental study of chevron, corrugated plate heat exchangers", *International Communications in Heat and Mass Transfer* 37 (2010) 1009-1014.
- [15] Sanjeev Jain and P.K. Bansal, "A new approach to numerical simulation of small sized plate heat exchangers with chevron plates", *Journal of Heat Transfer by ASME* Vol 129, March 2007.
- [16] Jonghyeok Lee and Kwan-Soo Lee., "Flow characteristics and thermal performance in chevron type plate heat exchangers", *International Journal of Heat and Mass Transfer* 78 (2014) 699-706, 2014.
- [17] Salman Al Zahrani and Feng Xu, "Thermal performance investigation in a novel corrugated plate heat exchanger", *International Journal of Heat and Mass Transfer* 148 (2020) 119095.
- [18] A.G Kanaris and V Paras, "Flow and Heat Transfer in Narrow Channels with Corrugated Walls a CFD Code Application", *Chemical Engineering Research and Design* 83(A5) 460-469,2017.
- [19] R. Gugulothu and E.L. Adithya, "A review on enhancement of heat transfer techniques", *Mater. Today Proc.* 4 (2) (2017) 1051–1056.
- [20] Ansys, "Ansys fluent 12.0 user guide" (2009).
- [21] B.SwaminAdhan and B.Sreedhara Rao, "Optimization of corrugation angle for the heat transfer performance of corrugated plate heat exchanger" *IRJET* ISSN: 2395-0056.
- [22] Mohd. Sohail Ansari and Prof.P.N. Awachat, "Heat transfer analysis of corrugated type Heat exchanger over coil type heat exchanger: A review" *IJRET* ISSN: 2278-0181 Vol: 3, Issue 3, March 2014.
- [23] E. Elshafei and E. El-Negiry, "Heat transfer and pressure drop in corrugated channels", *Energy* 35 (1) (2010) 101–110.
- [24] G. Longo and A. Gasparella, "Refrigerant r134a vaporisation heat transfer and pressure drop inside a small brazed plate heat exchanger", *Int. J. Refrig.* 30 (5) (2007) 821–830.
- [25] B. Thonon, "Design method for plate evaporators and condensers" in: *Proceedings of the BHR Group Conference Series Publication, Mechanical Engineering Publications Limited, 1995.*

BIOGRAPHIES



"Mr. Benny T. K
Assistant Professor, Department of Mechanical Engineering, RIET, Thiruvananthapuram, Kerala."



"Akhil A
UG Student, Department of Mechanical Engineering, RIET, Thiruvananthapuram, Kerala."



"Devakrishna A
UG Student, Department of Mechanical Engineering, RIET, Thiruvananthapuram, Kerala."



"Ramzy R
UG Student, Department of Mechanical Engineering, RIET, Thiruvananthapuram, Kerala."



"Sinan T
UG Student, Department of Mechanical Engineering, RIET, Thiruvanthapuram, Kerala."